Available online at www.sciencedirect.com

SCIENCE DIRECT®

Nuclear Instruments and Methods in Physics Research A 559 (2006) 676–679

NUCLEAR INSTRUMENTS & METHODS IN PHYSICS RESEARCH Section A

www.elsevier.com/locate/nima

Quasiparticle dynamics and a new, high-resolution readout of STJ photon detectors

Daniel E. Prober*, John D. Teufel, Luigi Frunzio, Christopher M. Wilson, Robert J. Schoelkopf

Department of Applied Physics, Yale University, P.O. Box 208284, 15 Prospect St.-Rm. 401, New Haven, CT 06520-8284, USA

Abstract

Quasiparticle dynamics and energy resolution of STJ single-photon detectors are described. A new readout, the RF-STJ, is presented and its implementation as an mm-wave detector is tested using an on-chip hot–cold source.

PACS: 84.40; 07.57.K; 85.25.P; 42.79.P

Keywords: STJ detector; Terahertz detector; mm-wave detection

1. Introduction

Superconducting tunnel junction (STJ) detectors have been developed over the past two decades as leading detectors of single photons for astronomical and spectroscopic measurements [1–5]. The basic operation of these devices has been reviewed, with mechanisms limiting the performance [5–7]. Here we review new results for understanding the performance, and a new method for reading out these devices, the RF-STJ, that is simple and has straightforward multiplexing [8,9].

The basic operation of the STJ detector is shown in Fig. 1. A photon of energy $\geqslant 0.1\,\mathrm{eV}$ is absorbed in the Ta film, breaking Cooper pairs and creating quasiparticles. These diffuse and enter the Al film, are trapped by phonon energy loss, and in a few microseconds they tunnel to the right electrode. If the bias energy eV is larger than the energy of the quasiparticle above the Al gap energy, the tunneling will occur only as an electron [6]. If the quasiparticle on the right is confined near the barrier, it can tunnel back to the Al trap. If it has lost energy $\approx$eV on the right side, it can tunnel back only as a hole, which adds to the charge in the forward direction. This backtunneling process is achieved by having a Ta contact on the right [5,10,11]—‘bandgap engineering’, or by constricting the path for diffusion away from the barrier—‘diffusion engineering’ [12]. The charge collected is larger for improved S/N, but it is slower than the single tunnel process in Fig. 1.

The best performance obtained in various energy ranges is shown below; the detection of alpha particles was accomplished by deposition of energy into a crystal substrate, and collection of the resulting phonons by the STJ. The TUM detector is on a SiN membrane. δE is explained in some cases [13,14,17] (Table 1).

2. Dynamic properties

Predicting STJ dynamic behavior involves a large number of issues and parameters. An important example of the intrinsic behavior is the quasiparticle recombination time in Al [10]. Measurement of noise due to quasiparticle number fluctuations show that the recombination in our Al films is due to intrinsic self-recombination of the quasiparticles. This is important for designing the device performance, because this recombination time sets an

---

*Corresponding author. Department of Applied Physics, Yale University, POB 208284, 15 Prospect St.-Rm. 401, New Haven, CT 06520-8284, USA

E-mail address: daniel.prober@yale.edu (D.E. Prober).

0168-9002/$ - see front matter © 2006 Elsevier B.V. All rights reserved.
doi:10.1016/j.nima.2005.12.101

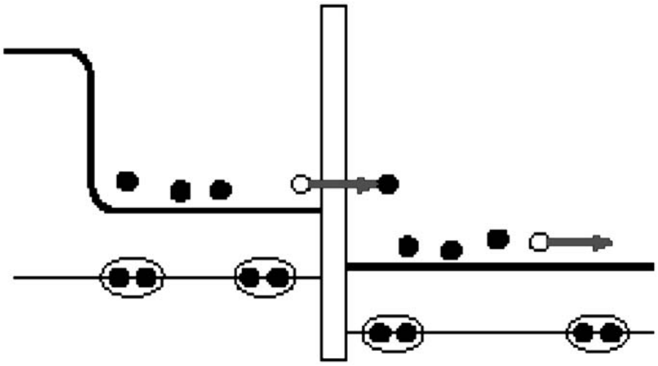

Fig. 1. STJ detector, single-tunnel process. The Ta gap = 0.7 meV on left is larger than Al = 0.18 meV.

Table 1
Best performance reported for STJ detectors

	E_{ph}(eV)	δE_{fwhm}	Group	Refs.
X-ray	5.9 k	13,12.4	Yale,TUM	[13,15]
EUV	70	1.7	LLL	[16]
Visible	2.5	0.1	ESA	[17]
Alpha	5.4 M	0.4%	RIKEN	[18]

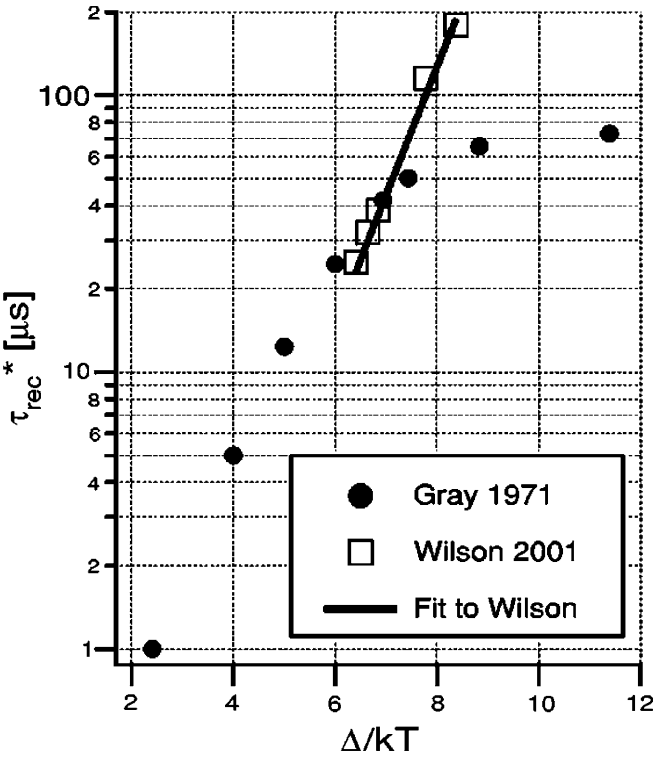

Fig. 2. Quasiparticle recombination time τ_{rec}* in Al [10,19]. In the Gray work, the time saturated for low T due to recombination at flux lines in the film.

upper limit to how long the quasiparticles are available to tunnel and contribute to the charge signal (see Fig. 2).

The long lifetime and weak phonon emission in Al [10,19] cause large heating effects in backtunneling devices with Ta contacts[10,20]. The quasiparticle lifetime is shorter in Ta [13] and in Ta/Al bilayers [11,21], and much shorter in Nb and Nb/Al bilayers [22]. In these, the trap states fill and empty on different timescales, so that the energy response of STJs that use such bilayer films varies with energy [11,22], unlike our single-tunnel devices.

3. RF-STJ multiplexed readout and mm-wave tests

An FET readout amplifier provides good sensitivity for optical thru X-ray energy for backtunneling devices, but limits resolution for single-tunnel optical devices [10]. Moreover, the number of STJs employed is limited by the complexity of connecting to FET amplifiers. SQUID amplifiers are not sensitive enough for the high impedance devices. A partial solution is to use 'one-dimensional' absorber strips, where the position of photon absorption is determined from the ratio of the two charge outputs from opposite ends. Trapping and charge division has been modeled in detail [13,23].

Development of an on-chip cold amplifier for use with the high impedance STJ can be done with the rf-SET readout [9,24], explored at Yale. The rf-SET in this application is extremely sensitive and fast, but is relatively complex. However, it does offer the ultimate sensitivity, so that even single photons of energy 1–10 meV should be detectable [25]. Photon counting in the mm-THz region would be desired in advanced space observatories with direct detectors for high spectral resolution [26].

A new readout method has been explored at Yale by Teufel et al. [8]. It uses the same microwave reflection method invented at Yale for reading out the very high impedance (>50 kΩ) of the SET [9,27]. This readout method is illustrated in Fig. 3. We have first tested the readout with an STJ where quasiparticles are produced by the absorption of a stream of mm-wavelength photons, directly into the Al absorber. We expect a response of 2 electrons per absorbed photon. The on-chip Au hot–cold noise source is coupled by a transmission line to the Al absorber; the Au wire emits as a 1D blackbody. For a uniform temperature, the spectral density of absorbed power is $P(f,T_{\mathrm{Au}}) = hf/(e^{hf/kT}-1)$ when coupled to a matched load. This reduces to Johnson noise, $P(f) = kT_{\mathrm{Au}}$ at low frequency. The temperature profile $T_{\mathrm{Au}}(x)$ along the length of the Au emitter is accurately computed from V_{Au} using diffusion cooling [28]. The power at a specific frequency is then given by integrating $P(f,T_{\mathrm{Au}}(x))$ along the length of the Au wire. The absorption of power by the Al absorber occurs only above f_{gap} of the Al, about 130 GHz for this dirty Al strip. To compute the absorbed power, we calculate the impedance match at each frequency above f_{gap} and integrate vs. f, using the Mattis–Bardeen result for the Al wire impedance. The Nb electrodes confine quasiparticles to the Al wire, with little or no loss.

The measured performance demonstrates that our design goals have been met. The measured response is

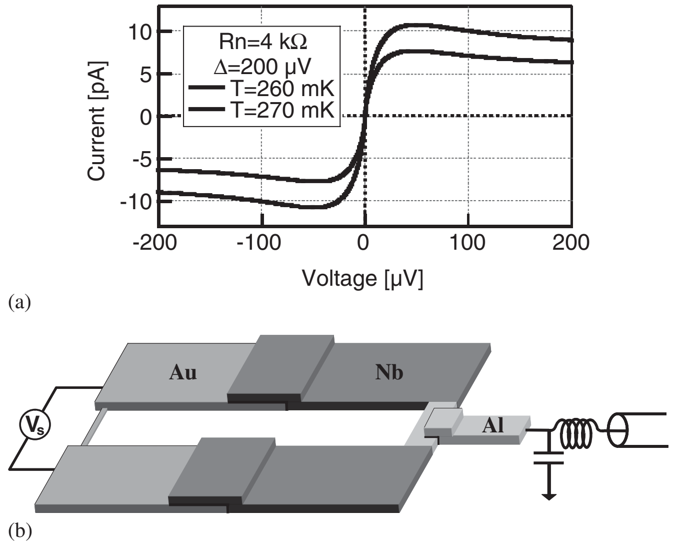

Fig. 3. (a) STJ IV around $V = 0$ at two different temperatures, showing the effect of excess quasiparticles in the Al. (b) Test system: Au hot–cold noise emitter, coplanar stripline with DC-blocking capacitors, and Al absorber, $R_{\mathrm{Au}} \approx R_{\mathrm{Al,n}} \approx 50\,\Omega$. The resonant readout couples the STJ $V \approx 0$ resistance (≈ 10–$50\,\mathrm{k\Omega}$) to the $50\,\Omega$ coaxial cable. A directional coupler and low noise cryogenic HEMT amplifier are used.

$R = 1700\,\mathrm{A/W}$, compared to a computed response of about $3000\,\mathrm{A/W}$. The difference is less than a factor of 2, and may be due to our imperfect knowledge of the exact gap frequency of the Al absorber, since the $P(f)$ is exponentially decreasing as $e^{-hf/kT}$ above f_{gap}. Also, it is possible, though unlikely [29], that some of the photons escape into free space. With the *measured* response, R, we find

$$\mathrm{NEP}^{\mathrm{OPTICAL}} = 1 \times 10^{-16}\,\mathrm{W/(Hz)^{1/2}}.$$

This is quite good for a device operating at 0.25 K, with a relatively large tunnel junction, $A = 2.5\,\mu\mathrm{m}^2$. This is one of the very first tests of an *OPTICAL* NEP of a microbolometer—one which is coupled to an antenna or to a transmission line. Most detector tests of such devices obtain an electrical NEP, but do not check directly the photon response. Our on-chip photon source is simple and allows us to exclude stray photons which could easily contaminate such a measurement.

The noise for this STJ is current noise due to the noise of the cryogenic HEMT amplifier as coupled through the resonant circuit. This sets the present level of NEP. The response time of the STJ is fast, $< 10\,\mu\mathrm{s}$ in this example, as limited by the tunnel time. This could be engineered to be faster. The bandwidth response of the resonant readout is of order 10 MHz in this example ($\approx 0.1\,\mu\mathrm{s}$), as determined by the $Q \approx 30$ and the drive frequency, 350 MHz. Thus, we can read out the STJ signal rapidly. Moreover, the resonant readout allows one to drive multiple STJs each with its own resonant readout, and use a single cryogenic HEMT amplifier to read all these detectors. Thus, the route is now open to frequency multiplexing the STJ devices in an efficient fashion. Much background research necessary for designing L and C multiplexing systems with on-chip components has been explored by Stevenson et al. [9] in the context of a similar readout approach for multiplexed rf-SETs.

The on-chip source of mm-wave photons is a new development also, and allows testing that is very flexible, with negligible extraneous noise. (All DC lines are rf filtered.) This source can be combined with on-chip high-Q resonant filters to produce relatively narrow band noise, to test, e.g., the frequency-dependent responsivity of our detectors. The source can be modulated very rapidly, with thermal time response $< 0.1\,\mathrm{ns}$ [28].

The RF-STJ presented detects power in the range 0.1–0.5 pW, appropriate for the relatively wide bands envisioned for a CMB polarization instrument [26]. Lower power applications require smaller STJs, and possible a lower operating temperature, $< 0.25\,\mathrm{K}$. We have tested small STJs at lower temperatures, and achieved DC currents below 10 fA, compared to the $\approx$nA thermal current of the present devices. The smaller current allows much smaller shot noise, and larger Q for the rf circuit. We project that $\mathrm{NEP} \approx 1 \times 10^{-18}\,\mathrm{W/(Hz)^{1/2}}$ can be achieved. Tests of this are in progress.

Acknowledgements

The research reported for Yale was conducted in collaboration with J. Teufel, M. Shen, C. M. Wilson, L. Frunzio, R.J. Schoelkopf, and T.R. Stevenson. We thank our other past Yale and GSFC collaborators. The research was supported by NASA, NASA-GSRP, and NSF DMR and AST.

References

[1] F. Gatti (Ed.), Nucl. Instr. and Meth. A, 520, 2004.
[2] F.S. Porter, et al. (Eds.), AIP Conf. Proc., 606, 2002.
[3] P. Verhoeve, et al., Proceedings of the ISCO SP-554 (2004) 781 as ESA 2004/SCI-A/30.
[4] S. Friedrich, et al., Rev. Sci. Inst. 73 (2002) 1629.
[5] N. Booth, D. Goldie, Supercond Sci.Technol. 9 (1996) 493.
[6] K. Segall, et al., Phys. Rev. B70 (2004) 214520;
K. Segall, et al., Phys. Rev. B64 (2001) 180508.
[7] G. Brammertz, et al., IEEE Trans. Appl. Supercond. 11 (2001) 828.
[8] J. Teufel, Yale University, unpublished.
[9] T.R. Stevenson, et al., Appl. Phys. Lett. 80 (2002) 3012.
[10] C. Wilson, et al., Phys. Rev B 69 (2004) 094524;
C. Wilson, et al., AIP Conf. Proc. 605 (2002) 145.
[11] A.G. Kozorezov, et al., Phys. Rev. B 69 (2004) 184506.
[12] V. Savu, et al., IEEE Trans. Appl. Supercond. 15 (2005).
[13] L. Li, et al., IEEE Trans. Appl. Supercond. 11 (2001) 685;
L. Li, et al., AIP Conf. Proc. 605 (2002) 145.
[14] A. Kozorezov, et al., Phys. Rev. B 69 (2004) 184506 and refs.
[15] G. Angloher, et al., AIP Conf. Proc. 605 (2002) 23.
[16] S. Friedrich, et al., IEEE Trans. Appl. Supercond. 9 (1999) 3330.
[17] P. Verhoeve, personal communication, 2005 and Nucl. Instr. and Meth A, this conference.
[18] M. Kurakado, et al., Appl. Phys. Lett. 86 (2005) 083503.
[19] S. Kaplan, et al., Phys. Rev. B 14 (1976) 4854.
[20] G. Brammertz, et al., SPIE 5499 (2004) 269.
[21] P. Verhoeve, et al., Nucl. Instr. and Meth A 520 (2004) 246.

[22] A. Poelaert, et al., Phys. Rev. Lett. 82 (1999) 1257.
[23] M. Ejrnaes, et al., Supercond. Sci. Technol. 18 (2005) 953.
[24] T.R. Stevenson, et al., IEEE Trans. Appl. Supercond. 11 (2001) 692.
[25] R.J. Schoelkopf, et al., IEEE Trans. Appl. Supercond. 9 (1999) 2935.
[26] T.R. Stevenson, Nucl. Instr. and Meth A, this conference.
[27] R.J. Schoelkopf, Science 280 (1998) 1238.
[28] D.E. Prober, Appl. Phys. Lett. 62 (1993) 2119.
[29] E. Wollock, personal communication, 2005.